1 Introduction

In eukaryotes, membranous organelles segregate and organize the vast array of intracellular biochemical processes. The compartmentalization of cells by membranes controls the selective exchange of matter and information between the two aqueous compartments the membranes separate. Membranes are therefore the basis for cellular development and differentiation in higher organisms (see Figure 1.1).

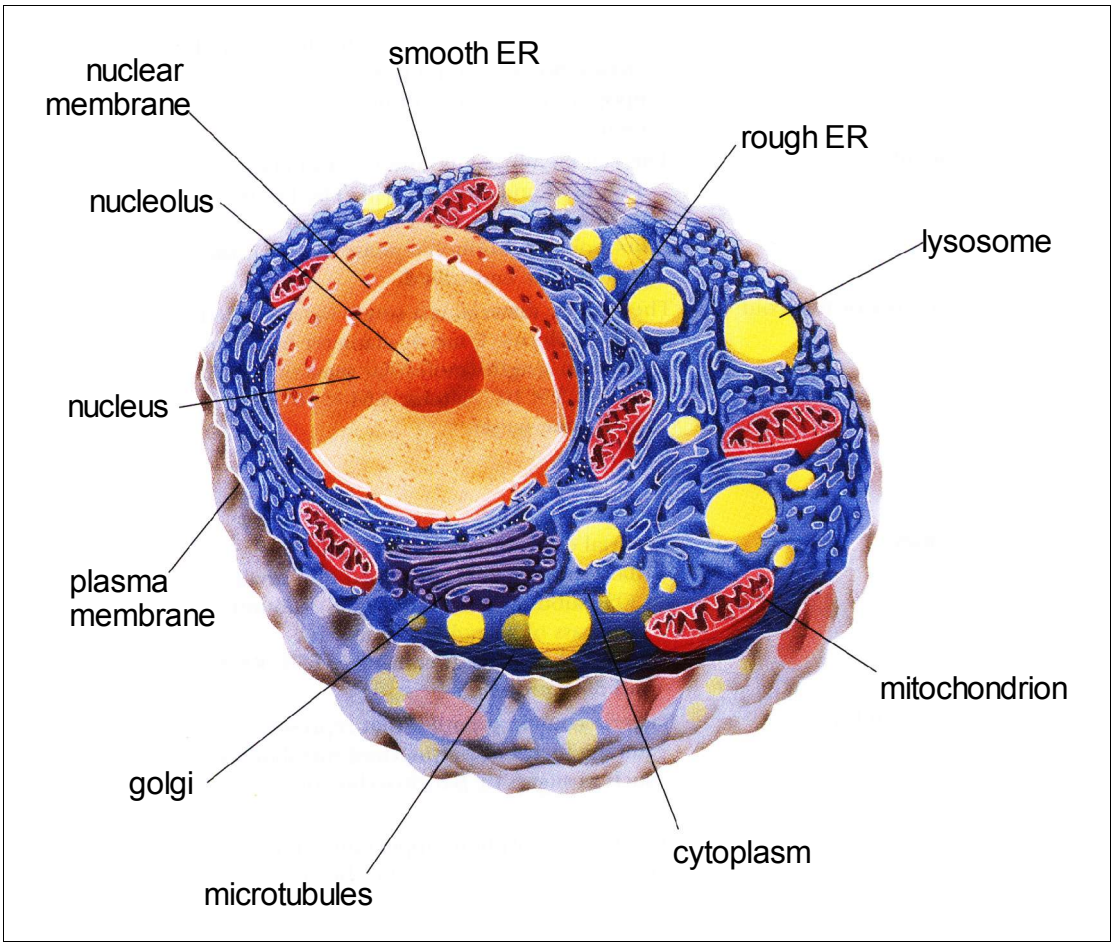

Figure 1.1: Diagram showing the characteristic features of a typical eukaryotic cell (rat). Note the different organelles made up by membranes. Modified from (Garrett and Grisham, 1998).

The primary function of a membrane is to pose as a barrier between two aqueous compartments. This raises fundamental questions for the movement of macromolecules from one compartment to another:

1. How are macromolecules transported across a membrane that normally would prevent such a movement?

2. How is the permeability barrier for ions maintained while selected macromolecules are transported across a membrane?

In response to these challenges, cells of higher organisms have developed complex molecular targeting and transportation machineries that provide the means for specific and unidirectional transport of macromolecules and ions.

1.1 Protein Transport across the Membrane of the Endoplasmic Reticulum

Protein biosynthesis is a central biological process in all living cells. All protein synthesis occurs in the cytoplasm of the cell. Ribosomes are the macromolecular assemblies responsible for mRNA translation in the cytosol of cells. They are large RNA-protein complexes that are built of two unequal subunits that perform the mRNA directed biosynthesis of polypeptides. They were first identified in cells by Palade at the Rockefeller University using electron microscopy (EM) (Palade, 1955).

The universal problems of macromolecular transport across membranes also apply to the transport of proteins: a substantial fraction of the polypeptides synthesized by ribosomes in the cytosol must either be integrated into or transported across membranes. The most extensive membranous network in higher eukaryotic cells is the endoplasmic reticulum (ER) which was discovered using EM by Porter, Claude, and Fullam at the Rockefeller

University (then Institute) in 1945 (Porter et al., 1945). The rough ER is studded with ribosomes and is the site of protein synthesis. The smooth ER is devoid of ribosomes and is, besides other functions, the major site of lipid synthesis.

In a process referred to as protein translocation, nascent chains destined for either membrane integration or secretion are specifically targeted to the ER and translocated across the ER membrane.

1.1.1 The Signal Hypothesis

Early studies of secretory pathways in eukaryotes revealed that mRNA coding for secretory proteins are translated on rough microsomes. Blobel and Sabatini postulated as early as 1971, that the nascent chain translation product of secretory or integral membrane proteins and not the mRNA itself would interact with the ER (Blobel and Sabatini, 1971). The suggested mechanism included as a prerequisite the existence of an amino-terminal signal sequence in the nascent chain that was postulated to be recognized by a soluble factor in the cytoplasm which then would bind the ribosome-nascent chain (RNC) complex to the ER. Blobel and Dobberstein then hypothesized in 1975, that secretory proteins are translocated through aqueous channels formed by integral ER membrane proteins (Blobel and Dobberstein, 1975a). For many years the concept of aqueous protein conducting channels in the ER membrane has been the matter of vigorous debate. The unifying principles proposed in the signal hypothesis still hold to this day:

- Nascent proteins carry intrinsic specific targeting signals at their amino termini.
- The targeting signals are recognized by selective signal receptors that are coupled to the ER membrane.
- Nascent polypeptides are transported through aqueous channels in the ER membrane.

1.1.2 Cotranslational Protein Transport

In 1975, Blobel and Dobberstein found that the signal sequence is cleaved off cotranslationally, suggesting a strictly cotranslational process for protein translocation across the ER membrane (Blobel and Dobberstein, 1975a). Cotranslational protein transport is the most common form of protein transport in higher eukaryotic cells and is divided into two distinct steps. The intrinsic signal sequence of the emerging nascent chain is first recognized and bound by a soluble factor in the cytoplasm. In 1980, Walter and Blobel identified the soluble factor in the cytosol that recognizes and binds the signal sequence and named it the signal recognition protein (Walter and Blobel, 1980), which was later renamed to signal recognition particle (SRP) when its essential 7S RNA component was discovered (Walter and Blobel, 1982). In a second step, the SRP and its membrane bound receptor (SR) target the SRP-RNC complex to the ER membrane (Gilmore et al., 1982a). The SRP and SR represent a ubiquitous protein targeting system whose basic concept is conserved in all organisms (reviewed in Keenan *et al.*, 2001).

The SRP subunit SRP54 recognizes and binds to the signal sequence of the nascent chain presented by the ribosome nascent chain complex (RNC) (Walter and Blobel, 1980; Walter and Blobel, 1982). The interaction between the RNC and the SRP leads to a translation slowdown that allows for the targeting of the RNC-SRP complex to the ER membrane (Walter et al., 1981). The interaction between SRP54 and the membrane bound SRP receptor (SR) selectively targets the RNC-SRP complex to the ER membrane (Gilmore et al., 1982a; Gilmore et al., 1982b; Meyer and Dobberstein, 1980b). This is followed by the release of the signal sequence from SRP54 and its insertion into the protein-conducting channel (PCC) that is formed by the oligomeric assembly of the trimeric Sec61p complex. Once the SRP dissociates from the RNC, translation resumes, and the nascent chain translocates into the ER lumen while the ribosome remains attached to the PCC (reviewed in Keenan *et al.*, 2001; Schnell and Hebert, 2003).

1.1.3 Posttranslational Protein Transport

In 1986, Waters and Blobel found that certain proteins can be translocated in a posttranslational process (Waters and Blobel, 1986). Such proteins are completely translated and are kept in a soluble state in the cytosol with the help of chaperones, before being targeted to the ER membrane (Chirico et al., 1988). Targeting and translocation of these nascent chains are not dependent on the SRP and require ATP. Although translocation still occurs through the Sec61p complex, there are additional four proteins associated with the Sec61p hetero-trimer (Sec62p, Sec63p, Sec71p, and Sec72p) to accomplish posttranslational proteins transport (Panzner et al., 1995). This complex is termed the heptameric complex.

1.1.4 Components of the Protein Targeting and Translocation Process

1.1.4.1 The Ribosome

The ribosome consists of three ribosomal RNAs (rRNAs) and 50-80 ribosomal proteins that form its subunits. The two subunits are referred to according to their sedimentation coefficients. The prokaryotic ribosome (70S) consists of a small (30S) and a large (50S) subunit with an overall molecular weight of 2.52 MDa. The eukaryotic ribosome (80S) is larger and made up of a small (40S) and a large (60S) subunit with an overall molecular weight of 4.22 MDa (see table 1.1 and 1.2 for a comparison).

Biochemical and structural evidence supports the central if not essential role of RNA in the translational cycle. The recently solved crystal structures of the small subunit from Thermus thermophilius (Schlünzen et al., 2000; Wimberly et al., 2000) and that of the large 50S subunit from *Halophile archaebacterium* (Ban et al., 2000) support the

mounting evidence from biochemical studies that the ribosome is in fact an RNA-based machine.

	Ribosome	***Small subunit***	***Large subunit***
Sedimentation coefficient	70S	30S	50S
Mass (kDa)	2520	930	1590
Major RNAs	-	16S = 1542 nt	23S = 2904 nt
Minor RNAs	-	-	5S = 120 nt
RNA mass (kDa)	1664	560	1104
RNA proportion	66%	60%	70%
Number of proteins	-	21 polypeptides	31 polypeptides
Protein mass (kDa)	857	370	487
Protein proportion	34%	40%	30.00%

Table 1.1: Structural organization and composition of the prokaryotic ribosome (*E. coli*, from (Garrett and Grisham, 1998))

	Ribosome	***Small subunit***	***Large subunit***
Sedimentation coefficient	80S	40S	60S
Mass (kDa)	4220	1400	2820
Major RNAs	-	18S = 1874 nt	28S = 4718 nt
Minor RNAs	-	-	5.8S = 160 nt 5S = 120 nt
RNA mass (kDa)	2520	700	1820
RNA proportion	60%	50%	65%
Number of proteins	-	33 polypeptides	49 polypeptides
Protein mass (kDa)	1700	700	1000
Protein proportion	40%	50%	35%

Table 1.2: Structural organization and composition of the eukaryotic ribosome (Rat, from (Garrett and Grisham, 1998))

Most of the information that exists today regarding the ribosome was gathered by studying the prokaryotic translation system. Evolutionary conservation allows one to anticipate that the fundamental mechanisms of protein biosynthesis are the same in eukaryotes. However, there are significant differences between the prokaryotic and the eukaryotic ribosome. The eukaryotic ribosome is much larger than the prokaryotic ribosome, which is not only due to the presence of more than 20-30 additional proteins (Witmann-Liebold, 1986; Wool et al., 1990 and Planta and Mager, 1998), but also to insertion elements in the rRNA (Gerbi, 1996).

1.1.4.2 Eukaryotic Protein Biosynthesis

The process of protein biosynthesis is divided into three steps: initiation, elongation, and termination (Garrett and Grisham, 1998). Both initiation and termination are special steps that are directed by specific mRNA codons (start- and stop-codons). Eukaryotic mRNA is characterized by two posttranscriptional modifications: the 5'-^{7}methyl-GTP cap and the poly(A) tail. The 5'-^{7}methyl-GTP cap is essential for ribosomal binding and increased stability of the mRNA while the poly(A) tail increases the stability of the mRNA and enhances translation efficiency.

Initiation

The initiator tRNA forms the so-called 43S preinitiation complex by binding to three initiation factors (eIFs) and the small ribosomal subunit (40S). Next, the 43S preinitiation complex binds the mRNA at its ^{7}methyl-GTP cap and the 48S preinitiation complex is formed upon binding of an additional four eIFs. The 48S pre-initiation complex moves to the start codon (AUG) and is bound by the large ribosomal subunit (60S), which triggers the release of the eIFs to form the 80S initiation complex.

Elongation

Ribosomes contain three tRNA-binding sites: the aminoacyl site (A site), the petidyl site (P site) and the exit site (E site). Following peptide bond formation the ribosome has a deacylated tRNA in the P site and a peptidyl tRNA in the A site. The A site has to be vacated in order to bind the next aminoacyl-tRNA. According to the “hybrid states model” (Moazed and Noller, 1989), the movement of the tRNA on the ribosome is to occur in two steps: In the first step, which occurs spontaneously after the peptidyl transferase reaction, the acceptor end of the deacylated tRNA and the peptidyl tRNA move relative to the large ribosomal subunit from the P and A site, respectively. Their anticodon ends remain bound to the small subunit resulting in P/E and A/P hybrid states. In the second step, the anticodon arms of both tRNAs move relative to the small subunit from the P and A sites to the E and P sites, respectively. At the end of translocation the deacylated tRNA is in the E site and the peptidyl tRNA is in the P site. This second step is dependent on an elongation factor (EF-G) that drives the translocation of the tRNAs by GTP hydrolysis.

Termination

Termination is dependent on GTP and the eukaryotic release factor (RF). Once the ribosome encounters a stop codon in the mRNA, RF·GTP binds to the A site. GTP hydrolysis leads to the hydrolysis of the peptidyl-tRNA ester bond and the release of the mRNA, the nascent chain, and the deacylated tRNA from the ribosome.

1.1.4.3 The Signal Recognition Particle

The functional core of the SRP consists of the signal sequence binding subunit (SRP54 in eukaryotes, Ffh in prokaryotes) and the SRP RNA molecule. This functional core is conserved in all kingdoms of life (reviewed in Keenan *et al.*, 2001) except in chloroplasts where the SRP lacks an RNA molecule altogether (Koch et al., 2003).

In higher eukaryotes, the SRP is a ribonucleoprotein consisting of six proteins (SRP9, SRP14, SRP19, SRP54, SRP68 and SRP72) which are bound to a 7S RNA. The SRP can be divided into two distinct domains that differ in their function. The hetero-dimer of SRP9 and SRP14 bind the Alu sequence of domain I of the SRP RNA to form the so-called Alu domain. The Alu domain is responsible for the translation slowdown. The Alu domain in yeast differs slightly from its mammalian homologue. Yeast, lacking a SRP9 homologue, utilizes an SRP14 homo-dimer in place of the SRP9/SRP14 hetero-dimer found in mammals. Additionally, the Alu domain of the yeast SRP-RNA lacks two helices found in the mammalian form. The other SRP domain is the so-called S domain and contains the SRP subunits SRP19, SRP54, SRP68 and SRP72 that bind to the remainder of the SRP RNA. The S-domain is required for signal sequence binding and the SRP-SR interaction .

The signal sequence binding protein SRP54 is related to Ras-like GTPases (reviewed in Keenan *et al.*, 2001). It is the protein component of the functional core of the SRP and consists of an amino terminal N domain, a central GTPase domain (G domain), and a C-terminal M domain. The N and G domains form a distinct structural element referred to as the NG domain (Freymann et al., 1997). The M domain is rich in methionine and responsible for the interaction with the SRP RNA as well as the recognition and binding of the signal sequence.

SRP itself is a rod-like structure approximately 5-6 nm in width and 23-24 nm in length as revealed by electron microscopy (Andrews et al., 1985).

1.1.4.4 The Signal Recognition Particle Receptor

SRP mediated elongation slowdown is abolished upon the addition of microsomal membranes. This finding led to the proposal of a membrane bound SRP Receptor (SR) (Gilmore et al., 1982a), which was later isolated from microsomal membranes. The SR is a hetero-dimer consisting of an α- and β-subunit. The larger SRα has a molecular weight of 69 kDa and is peripherally associated with the ER membrane by its interaction with the smaller SRβ subunit, which is an integral membrane protein of 27 kDa with one transmembrane segment. Both subunits bind GTP (Connolly and Gilmore, 1989) and are exclusively located at the ER membrane (Gilmore et al., 1982b).

The GTPase domains of SRP54 and SRα are very similar in structure and function. Structural studies of their prokaryotic homologues have shown that together with their eukaryotic homologues, they form their own family within the GTPase superfamily (Freymann et al., 1999; Montoya et al., 1997b). They are characterized by a low affinity for nucleotide and are all stable in their empty states. SRα binds to SRβ via its N-terminal "SRX-domain". The interaction between SRβ and the SRX domain is characterized by hydrophobic and hydrophilic interactions (Schwartz and Blobel, 2003).

The function of the GTPase domain of SRβ has long been a matter of conjecture. A recent structural and biochemical study showed that SRβ effectively binds SRα only when SRβ is bound to GTP and not when bound to GDP, revealing that the GTP cycle of SRβ controls the association and dissociation of the hetero-dimeric SR (Schwartz and Blobel, 2003).

SRβ is closely related to members of the ADP-ribosylation factor (ARF) GTPase family (Miller et al., 1995). ARFs are conserved in all eukaryotes and are involved in the regulation of vesicle transport (reviewed in Jackson and Casanova, 2000). SRβ contains a transmembrane segment providing the membrane anchor for SRα (Young et al., 1995). However, a truncated protein representing the cytosolic GTPase domain without the transmembrane domain is functional in protein targeting (Ogg et al., 1998). SRβ is

present only in eukaryotes. The prokaryotic SRα homologue FtsY is a hydrophilic protein that is mainly localized in the cytoplasm and only partially associates with the cytoplasmic side of the plasma membrane by interacting with anionic phospholipids (reviewed in Koch *et al.*, 2003).

1.1.4.5 The Protein Conducting Channel

Protein Conducting Channels (PCC) are composed of several ER membrane proteins that associate to form an aqueous pore through which secretory proteins and lumenal domains of membrane proteins pass from the cytoplasm to the ER lumen (reviewed in Johnson and van Waes, 1999; Schnell and Hebert, 2003). Recent studies have revealed that the PCC is a complex and sophisticated molecular machinery that regulates the movement of polypeptides through the lipid bilayer of the ER membrane. The PCC most likely also opens laterally to allow the insertion of newly synthesized integral membrane proteins into the ER membrane.

Components of the PCC were identified by genetic as well as crosslinking studies in which photo-reactive probes were incorporated directly into nascent chains. The PCC in eukaryotes is composed of an oligomeric assembly of hetero-trimeric integral membrane proteins: Sec61α, -β and -γ. In yeast there are two homologous α-subunits (termed Sec61p and Ssh1p) and two homologous β-subunits (termed Sbh1p and Sbh2p). The two α- and β-subunits form distinct trimeric complexes (termed the Sec61p- and Ssh1p complexes), each with the shared γ-subunit (termed Sss1p) (Görlich and Rapoport, 1993; Toikkanen et al., 1996 and Finke et al., 1996). In comparison to the Sec61p complex, the Ssh1p complex interacts with signal sequences of stronger hydrophobicity and appears to be involved exclusively in cotranslational protein transport (Wittke et al., 2002).

A cryo electron microscopy study of the non-translating ribosomes with a purified Triton X-100 solubilized trimeric Sec61p complex from yeast had shown that the Sec61p

complex binds to the large ribosomal subunit, where it perfectly aligns with the exit tunnel of the large ribosomal subunit (Beckmann et al., 1997). It thus appears that during cotranslational protein transport the nascent chain directly moves from the aqueous channel in the large ribosomal subunit into the aqueous pore in the ER membrane formed by the PCC. The 3-D structure showed a single connection between the PCC and the ribosome. Interestingly, the structure showed a gap between the channel and the ribosome. This gap was attributed to missing proteins, the non-active conformation of the ribosome and the lack of a signal sequence. A recent cryo-EM study of mammalian ribosome-Sec61 complexes reported a very similar spatial arrangement with several connections forming the ribosome-channel junction but still leaving a gap between the Sec61p complex and the ribosome (Menetret et al., 2000). This gap was observed with both purified Sec61 complexes and with native translocons purified from solubilized rough microsomes, even under conditions where a signal sequence was assumed to be present. This challenged the current view of seal formation between the ribosome and the channel (Menetret et al., 2000). It had been assumed before that the permeability barrier during protein transport is maintained by a tight ribosome-PCC seal preventing the uncontrolled flow of ions and smaller molecules during protein translocation (reviewed in Johnson and van Waes, 1999). It thus appears that the PCC itself might be able to maintain the permeability barrier. The gap between the PCC and the translating ribosome would also explain the accessibility of cytosolic loops in nascent chains to the cytosol as observed in protease protection assays.

Proteins in yeast can be translocated either cotranslationally or posttranslationally. The trimeric Sec61p complex which forms the PCC involved in cotranslational protein transport, can also associate with four additional subunits (Sec62p, Sec63p, Sec71p and Sec72p) to form the so-called heptameric complex (Panzner et al., 1995). The heptameric complex facilitates posttranslational protein transport in yeast independent of the SRP-SR targeting machinery. Mainly characterized in yeast, the length as well as the hydrophobicity of the signal sequence determines whether a nascent chain is translocated co- or posttranslationally. Signal sequences with longer and more hydrophobic cores show a more pronounced SRP dependency (Ng et al., 1996). Similar

to cotranslational protein transport, posttranslational protein transport occurs in two distinct steps. In the first step the signal sequence is recognized by the Sec62p/63p subcomplex and is delivered to the Sec61p complex within the heptameric complex. The subsequent translocation is thought to be driven by the sequential binding and release of Kar2p (BiP in mammals), binding to and subsequently releasing the nascent chain, an ATP driven reaction that provides the unidirectionality to the posttranslational protein transport reaction while at the same time providing a permeability barrier for the PCC (reviewed in Johnson and van Waes, 1999; Schnell and Hebert, 2003).

1.2 Guanine Nucleotide Binding Proteins – Molecular Switches

While ATP is the energy source for such processes as metabolic reactions of enzymes and the movement of motor proteins, GTP seems to be mostly used for regulation via guanine nucleotide binding proteins (GNBPs) with the notable exception of protein translation (reviewed in Vetter and Wittinghofer, 2001). GNBPs or GTPases describe a protein family of highly conserved molecular switches. They are involved in the regulation of many complex functions like cell cycling, cell growth and cell differentiation, protein trafficking and synthesis, and vesicular and nuclear transport. GTPases cycle between an “on” and an “off” state. Their activation requires the dissociation of GDP from the GTPase and the association of GTP with the notably exception of SRP54 and SRα which are stable in their empty forms (Bacher *et al.*, 1996; Miller *et al.*, 1993). The intrinsic dissociation of GDP is extremely slow under physiological conditions. In the cell this *switch-on* reaction is accelerated by guanine nucleotide exchange factors (GEFs). GEFs stabilize the energetically unfavorable “empty state” of a GTPase and thereby allowing the GTP to bind. The *switch-off* reaction involves the hydrolysis of GTP to GDP and is, in contrast to the *switch-on* reaction, irreversible. Hydrolysis of GTP is intrinsically slow as well and is accelerated by GTPase activation proteins (GAPs) (reviewed in Vetter and Wittinghofer, 2001).

1.2.1 Guanine Nucleotide Exchange Factors

The intrinsic release of guanine nucleotide from GNBPs is slow under physiological conditions and is accelerated by GEFs by several orders of magnitude. The GEF mechanism involves a series of reaction steps leading to the release of nucleotide by the GNBP. They lead from a binary protein-nucleotide complex to a binary nucleotide-free complex which is stable in the absence of nucleotide via a trimeric GNBP-nucleotide-GEF complex. This reaction is then reversed by the rebinding of nucleotide, usually GTP due to its higher concentration in the cell. This reaction is in principle reversible and the equilibrium is determined by the affinity of the GNBP for GTP or GDP, the intracellular concentrations of GTP and GDP, and the concentrations of other effectors forcing the equilibrium towards the GTP-bound form.

GEFs are usually conserved within a subfamily of GTPases. In the case of SRβ which is most closely related to the ARF family, the GEFs share a common functional region of about 200 amino acids, the Sec7 domain (reviewed in Jackson and Casanova, 2000). Although the details of the GEF-GNBP interactions are different for the subfamilies, they all share common structural features, suggesting mechanistic similarities. These similarities are based on the fact that the nucleotide binding sites share common features. Although structures of some GNBPs with their GEFs in their “empty state” have been solved, the order of events that lead to the release of the nucleotide still remain unclear (reviewed in Vetter and Wittinghofer, 2001).

1.2.2 The GTPase Cycle during Cotranslational Protein Targeting

1.2.2.1 Cotranslational Protein Transport is dependent on GTP

Cotranslational protein transport to the ER is controlled by the concerted interaction of three GTPases: the SRP54 subunit of the SRP and the α- and β-subunits of the SR.

SRP54 recognizes and binds the signal sequence, leading to a RNC-SRP complex (reviewed in Keenan *et al.*, 2001). SRP54 binds GTP when in contact with the RNC (Bacher et al., 1996). The interaction between SRP54 and SRα leads to the formation of a GTP stabilized SRP-SRα complex (Rapiejko et al., 1997). It is this step that targets the SRP-RNC complex to the ER membrane. After the signal sequence is transferred to the PCC, GTP hydrolysis dissociates the SRP-SRα complex (Connolly et al., 1991), with SRP54 and SRα serving as mutual GTPase-activating proteins (GAP), a reciprocally symmetric interaction that is unique among known GTPases (Powers and Walter, 1995). The GTP hydrolysis of SRβ dissociates SRα from SRβ, thus disassembling the hetero-dimeric SR complex (Schwartz and Blobel, 2003).

1.2.2.2 Signal Sequence Transfer to the PCC

The SRP-SR interaction couples the recognition of the signal sequence with the targeting and association of the RNC to the ER membrane. The precise order of events that lead to the disassembly of the RNC-SRP-SR complex and the transfer of the signal sequence from the RNC to the PCC remain to be elucidated.

1.3 Three Dimensional Electron Microscopy of Macromolecular Assemblies

Understanding biological processes in all their detail necessitates the study of these processes on a molecular level. Biological macromolecules form three dimensional structures based on their chemical composition and their environment within the cell. Techniques like X-ray crystallography and nuclear magnetic resonance (NMR) spectroscopy allow the structures of biological macromolecules to be determined on an atomic level. While X-ray crystallography covers the full range of small molecules to some very large macromolecular assemblies, the limiting factors of this technique are still expression, crystallization, and the stability and homogeneity of the structure. With NMR spectroscopy, structures can be determined in solution but the technique's main restriction is its limitation to structures smaller than 100 kDa (reviewed in Saibil et al., 2000).

1.3.1 Electron Microscopy

Electron microscopy fills the gap that is left by X-ray crystallography, which is able to achieve atomic resolution of biological macromolecules, and the light microscope, which is able to deliver images of very large biological particles or organelles (Frank, 1996). In order to obtain a three dimensional representation of a macromolecule using an electron microscope (EM), the initially hydrated molecule has to be stabilized so it can be put into the vacuum of the EM. The intrinsic contrast of biological samples is very low and usually not sufficient for direct observations of biological samples. Various methods have therefore been developed to not only stabilize biological samples for electron microscopy but also to increase the contrast.

1.3.1.1 Negative stain

The method of negative stain EM was introduced by Brenner and Horne. The aqueous solution of a sample is mixed with 1-2 % of uranyl acetate and applied to a carbon coated copper grid (Brenner and Horne, 1959). The structural information provided by an image obtained from a sample that was negatively stained is limited to the shape of the molecule in that particular projection since the stain can barley penetrate, if it can at all, into aqueous channels of the sample molecule ("specimen casting") (see Figure 1.2).

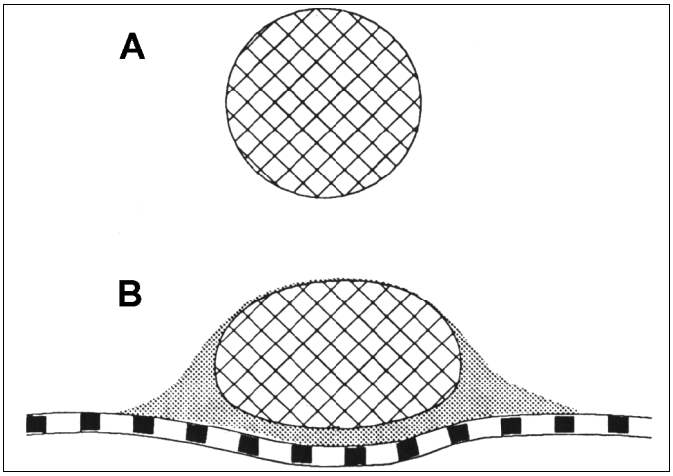

Figure 1.2: Representation of the effect of sample preparation on particle shape during negative staining. (A) Original shape of the particle in its fully hydrated state. (B) particle shape after negative staining on a single carbon surface.

Therefore an image of a negatively stained sample can provide no information about the interior of the specimen. In addition, the shape of the molecule is distorted due to air drying artifacts .

There are several artifacts that can be observed in negatively stained samples:

- the particle is flattened and surrounded by a minuscule of stain
- the staining is one-sided, so the top of the particle might be invisible in the projection
- the carbon surface shows an indentation at the location of the stained particle

However, negative stain is still a valid and suitable method in high resolution electron microscopy today. It can be used as a first step to provide characteristic views in order to evaluate if a sample is suitable for any other high resolution method.

1.3.1.2 Cryo Electron Microscopy

In cryo-Electron Microscopy (cryo-EM), the biological specimen is applied to a carbon coated copper grid in its native hydrated state. The excess of buffer is blotted away and the grid is rapidly plunged into liquid ethane at the temperature of liquid nitrogen (Figure 1.3). Due to the high heat conductivity of liquid ethane (> 10.000 K/second) and since the layer of water after blotting is very thin (200-2000 Å), the water is rapidly vitrified into a solid glass-like sheet of vitreous ice (freezing takes place in << 1 msec) with no crystals formed (Dubochet et al., 1988). Thus, the specimen is frozen in a close-to-native state and transferred like this in a special cryo-EM specimen holder into the cryo electron microscope. The grid is kept at liquid nitrogen temperature during the whole experiment and the image contrast observed is related to the biological specimen itself rather than to a contrasting agent.

Due to the rapid freezing of the sample, it is also possible to conduct time resolved experiments to capture very short-lived structural states of a specimen (Berriman and Unwin, 1994). The rapid freezing also prevents any collapsing of the structure and the embedding in vitreous ice also traps free radicals that are formed by the exposure of the specimen to the EM electron beam.

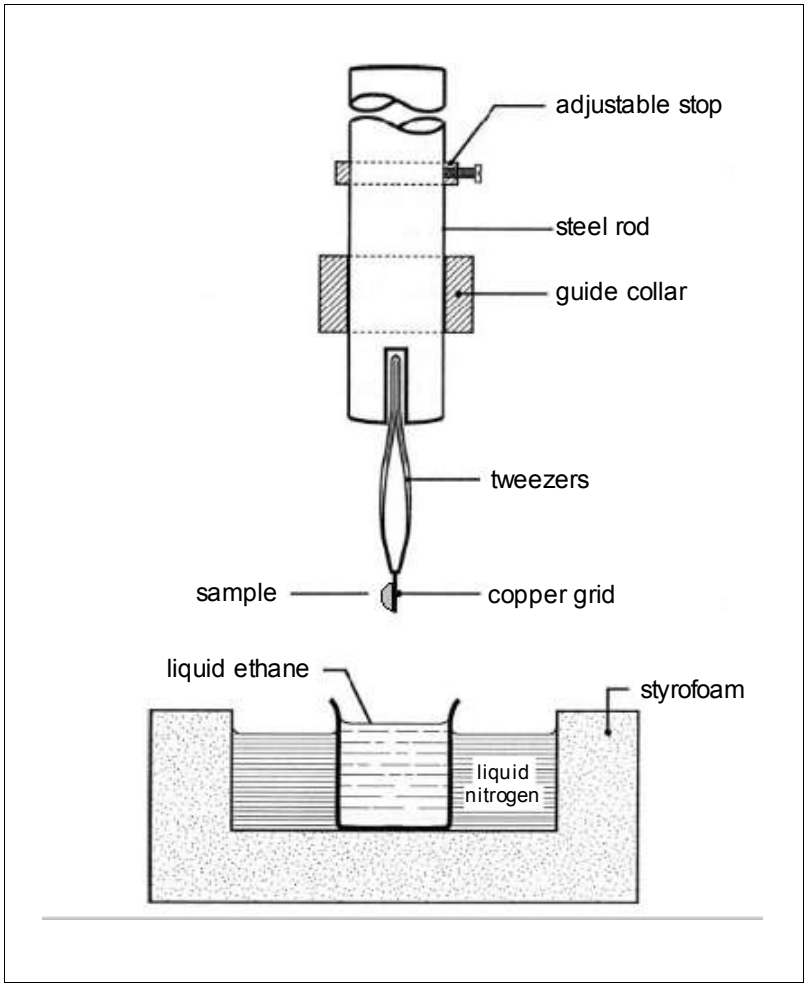

Figure 1.3: Vitrification of a cryo-EM specimen. A cryo-EM grid with a small film of sample solution is rapidly plunged into liquid ethane for vitrification using a plunging device.

1.3.2 Three Dimensional Reconstruction using Single Particle Analysis

In order to further limit the damage by radiation in the electron microscope, and to obtain useful information from the specimen, the electron dose during the experiment has to be kept extremely low. As a consequence of the low intensity of the electron beam and the very low intrinsic contrast between protein and water, the signal to noise ratio of the resulting images is extremely low. To extract information out of these images, some kind of averaging has to be performed to bring out the signal. Thus, the structures of may particles have to be averaged. This method was initially applied to (a) structures that are highly ordered and composed of symmetric arrangements of repeating elements (viruses with icosahedral symmetry) (Conway et al., 1997), (b) helical arrangements of proteins (acetylcholine receptor) (Miyazawa et al., 1999) and (c) two dimensional crystals (light harvesting complex) (Kuhlbrandt et al., 1994).

However, the real power of the method lies in applying it to macromolecules that occur in the form of isolated “single-particles”. This does not only extent the range of particles considerably but also brings out the full advantages of cryo-EM:

- a molecule is visualized e.g. in interactions with a ligand
- the interaction between the molecule and the ligand is free of interferences by crystalline packing
- theoretically, all naturally occurring states of the molecule are available for study

The goal of a three dimensional reconstruction by single particle analysis is to build a three dimensional model from two dimensional images. Cryo-EM in combination with single particle analysis provides three dimensional electron scattering density maps of macromolecules that are very similar to the electron density maps determined by X ray crystallography.

1.3.2.1 Image Formation in the Electron Microscope

The formation of an image in the electron microscope is an immensely complex process. Its basis is the interaction of electrons with the object (Frank, 1996). One can distinguish two different types of interactions: elastic and inelastic scattering. Elastic scattering does not involve a transfer of energy to the object, has a wide angular distribution and gives rise to high-resolution information. Inelastic scattering on the other hand, involves the transfer of energy to the object and causes radiation damage. Its angular distribution is narrow and leads to a low resolution background.

1.3.2.2 The Contrast Transfer Function

Thin samples of biological molecules fulfill the weak phase approximation, which is used to describe and analyze the phase contrast images of weakly scattering specimen (Frank, 1996).

The image formation in bright field electron microscopy can be described by the action of the contrast transfer function (CTF) $\mathrm{H}(\mathrm{k})$. Accordingly, the relationship between the object $\mathrm{o}(\mathrm{r})$ and the image contrast $\mathrm{i}(\mathrm{r})$ can be written as:

$$\mathrm{i}(\mathrm{r}) = \mathrm{o}(\mathrm{r}) * \mathrm{h}(\mathrm{r}) \qquad \text{(Formula 1.1)}$$

where * stands for the convolution operation, and $\mathrm{h}(\mathrm{r})$ is the point spread function, which is the Fourier transform of $\mathrm{H}(\mathrm{k})$. Thus, following the convolution theorem:

$$\mathrm{I}(\mathrm{k}) = \mathrm{O}(\mathrm{k})\mathrm{H}(\mathrm{k}) \qquad \text{(Formula 1.2)}$$

The shape of the CTF, $H(k)$, depends on several parameters:

- **defocus** - the deviation in the focus of the objective lens from the "Gaussian focus."
- **spherical aberration coefficient** - the (third order) spherical aberration of the wave front in the objective lens.
- **source size** - the illumination divergence, expressed as a size in the back focal plane (hence a quantity in reciprocal space).
- **defocus spread** - which describes the spread of defocus due to the spread of electron energies or to the fluctuation of lens current.

The only parameter being varied in the experiment is the defocus. Depending on the defocus setting, different features of the object appear enhanced or suppressed in the image. This is because the CTF oscillates between -1 (negative contrast transfer) and +1 (positive contrast transfer) as one goes from low to high spatial frequencies. The exact locations of the zero crossings (where no contrast is transferred and information is completely lost) depends on the defocus (Figure 1.4) (Frank, 1996).

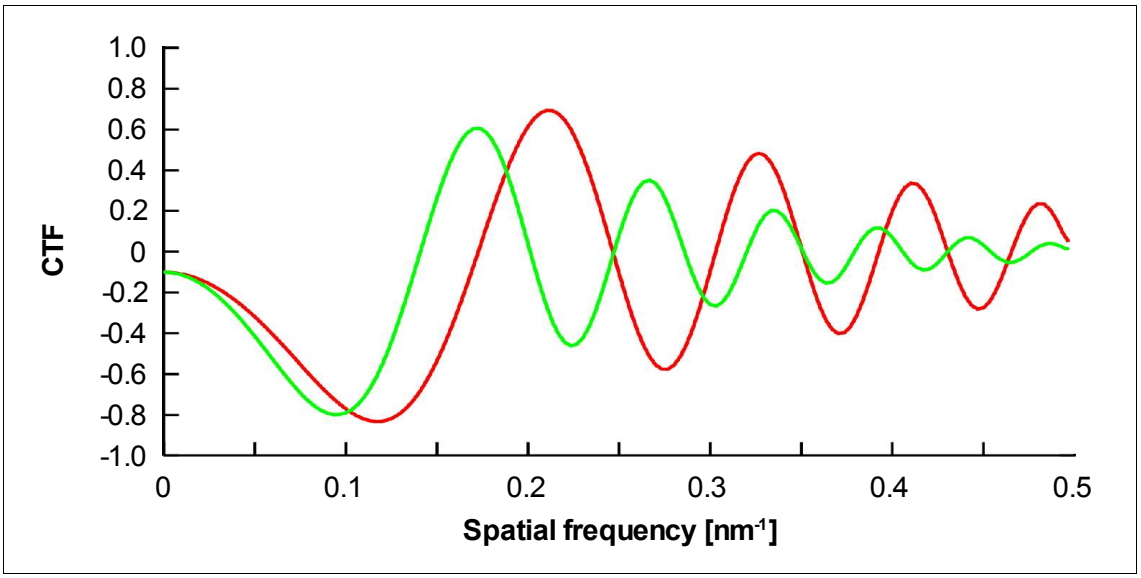

Figure 1.4: Defocus dependency of the CTF. The contrast transfer function (CTF) for two defocus values: 2.0 µm (red line) and 3.0 µm (green line). Note the shift of zero-crossing at different defocus values.

1.3.2.3 Contrast Transfer Function (CTF) Correction

The CTF describes the contrast transfer as a function of spatial frequency. It has alternating bands of positive and negative contrast seen in the scattering from carbon film as Thon rings (See Figure 1.5).

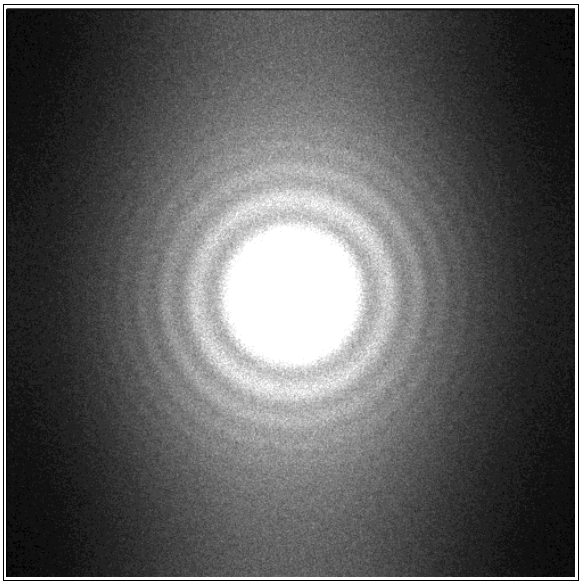

Figure 1.5: Thon rings. An averaged power spectra from a cryo-EM micrograph showing Thon rings from electron scattering of the carbon film.

Images have to be collected at a range of defocus to fill in the missing data from each caused by the zeros in the CTF which vary with defocus (compare Figure 1.4). In order to restore the corrected structural information, each image has to be corrected for the CTF.

1.3.2.4 Single Particle Analysis

The electron resolution of a modern transmission electron microscope is around 1Å. However, the practical resolution is restricted by the small aperture size of the EM that is needed due to aberrations in magnetic lenses.

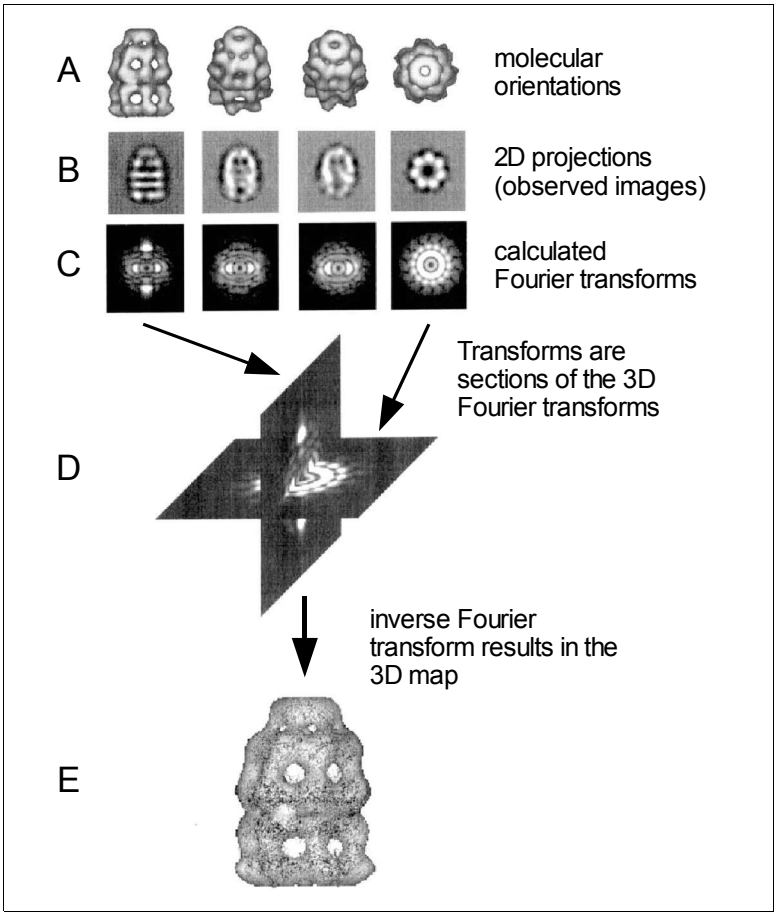

Figure 1.6: Principle of 3D reconstruction from 2D projections. (A) A set of surface rendered electron densities are shown above their corresponding 2D projections (B). (C) The Fourier transform of each 2D projection is a section through the 3D Fourier transform of the structure. (D) The 3D Fourier transform can be reconstructed by intersecting the transform sections. (E) the 3D electron density of the structure can be obtained by inverse Fourier transform. Modified from (Saibil, 2000).

A consequence of the small aperture is a large depth of field for each image taken using the small aperture. Therefore, the recorded images of macromolecular assemblies represent a 2D projection of the particles 3D density (reviewed in Saibil, 2000). Figure 1.6 illustrates the recovery of 3D densities from 2D projections.

Translational and rotational parameters to align 2D projections can be obtained by intersecting their Fourier transforms and cross-correlating them in Fourier space. An inverse Fourier transform of the aligned and combined Fourier transforms of the 2D projections then results in a 3D electron density map that, when surface rendered, represents the 3D structure of the particle.

1.3.2.5 Three Dimensional Reconstruction of Single Particle Specimens using Reference Projections

In the case of an existing reference structure, a structure can be refined by projection matching (Penczek et al., 1994). Figure 1.7 illustrates the process with a flow diagram.

A reference structure is reprojected using a defined set of initially coarse angular steps. The set of raw images is first cross-correlated with the set of projections from the reference structure to determine initial translational and rotational parameters for alignment. The new set of aligned images is used to generate an initial 3D map of the structure. This process is iterated through a refinement procedure, in which reference projections are obtained from the initially calculated structure using increasingly finer angular steps until the assignments converge. The convergence is usually judged by the stability of angle and projection assignments for each raw image. The iterative process of alignment searches by cross-correlation is extremely computationally intensive.

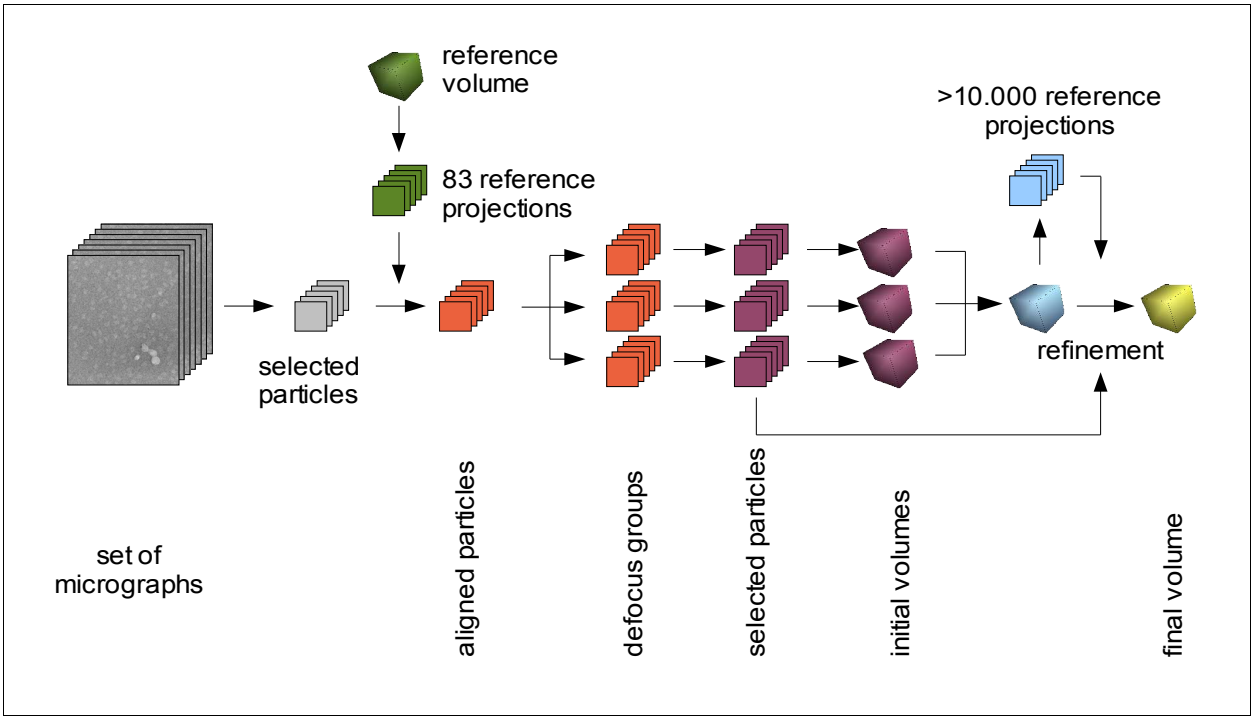

Figure 1.7:Flow diagram of a 3D reconstruction using projection matching. Raw images of single particles are obtained from recorded micrographs and aligned against reference projections that have been obtained from a reference structure. The raw images are aligned and segregated into groups according to their defocus. After a quality based selection process, the images of each defocus group are used to calculate an initial 3D structure per defocus group. The initial 3D structures are corrected for the contrast transfer function (CTF) and merged to result in an initial volume. The resolution of the initial volume is iteratively improved by a refinement procedure using a higher number of reference projections.

Higher resolutions can be achieved by analysis of a larger number of images which is limited by computer power. However, 3D electron densities of 3.5 Å resolution have been calculated (Henderson et al., 1990). Although theoretically possible, it has yet to be shown that the orientation refinement and optical corrections can be performed with a high enough accuracy to achieve atomic resolution from single-particle images.